SBF-1, a synthetic steroidal glycoside, inhibits prostate cancer cell growth through the blockade of mTOR and SIX1 interaction

Ahmed Elgehama [a], Lijun Sun [c, d], Biao Yu [c], Wenjie Guo [a, b], Qiang Xu [a, b, *]

[a] State Key Laboratory of Pharmaceutical Biotechnology, School of Life Sciences, Nanjing University, Nanjing, China.

[b] Jiangsu Key Laboratory of New Drug Research and Clinical Pharmacy, Xuzhou Medical University, 209 Tongshan Road, Xuzhou 221004, Jiangsu, China.

[c] State Key Laboratory of Bio-organic and Natural Products Chemistry, Shanghai Institute of Organic Academy, Shanghai 200032, China

[d] Department of Chemistry, University of Science and Technology of China, 96 Jinzhai Road, Hefei, Anhui 230026, China

[*]**Correspondence to** Qiang Xu, PhD.

State Key Laboratory of Pharmaceutical Biotechnology, School of Life Sciences, Nanjing University, Nanjing, 210023, China. Tel/Fax: +86-25-89687620; E-mail molpharma@163.com (Q. Xu)

Summary

The AR (androgen receptor) is a primary therapeutic target in androgen-dependent prostate cancer. Challenges remain for AR-independent prostate cancer as they exhibit complex cellular signaling in their progression rather than relying on the AR. Currently, prostate cancer metabolic signaling became an achievable target in prostate cancer treatment. In the present study, synthetic steroidal glycoside SBF-1, a potent anti-tumor agent known to have a strong cytotoxic effect on different kinds of cancers. We investigated SBF-1 potentials in AR-independent prostate cancer treatment and its effect on prostate cancer metabolic signaling. SBF-1 inhibited the growth of AR independent prostate cancer cell lines DU145 and PC3. Also, SBF-1 downregulates AKT/mTOR pathway and inhibited the ENO1 (alpha-enolase 1) protein and gene levels. Besides, SBF-1 blocked the interaction between mTOR and SIX1, which, for the first time shown mTOR essential for the regulation of ENO1 through binding to SIX1 (sineoculis homeobox homolog 1), accordingly, nuclear mTOR is an essential coregulator for the transcription of the ENO1 gene. Blocking the interaction between mTOR and SIX resulted in robust cell growth inhibition also the downregulation of ENO1, a consensus target in prostate cancer treatment. Accordingly, the current study suggests that SBF-1 is a leading compound in treating androgen-independent prostate cancer. Also, targeting the interaction between mTOR and SIX1 considered a better strategy in Androgen independent prostate cancer treatment.

Keywords: Prostate cancer; CRPC; SBF-1; mTOR; SIX1; ENO1

1. Introduction

Prostate cancer is considered remarkably fatal in men with estimated cases of more than 160,000 recorded cases in the united states, even though prostate cancer is a slowly progressing type of cancer, still considered the 3rd highest fatal cancer in men (*1*).

Targeting the androgen receptor (AR) and its signaling pathway is a primary strategy for prostate cancer treatment. At the same time, resistance occurs as the AR loses its function in the androgen depletion independent (ADI) prostate cancer. Androgen depletion independent prostate cancer has two types, type 1 does not express AR, and type 2 were AR become functional as an oncogene. PC3 and DU145 prostate cancer cell lines used in this study categorized as an early ADI type 1. Both PC3 and DU145 cell lines do not express AR and represent androgen-independent prostate cancer (*2*). The challenges remain regarding androgen-independent prostate cancer; thus, finding novel treatments became a severe need for scientists to discover. A well-reported anti-tumor small molecule, SBF-1, is a synthetic steroidal glycoside with a strong inhibitory effect against different types of cancer (*3-5*). SBF-1, as a steroid, strongly proposed its potential effect on cell metabolic signaling, and testing this small molecule could be feasible in the treatment of androgen-independent prostate cancer.

Taking advantage of previous studies that show early-stage prostate cancer relies on lipids and glutamine to sustain energy rather than aerobic respiration (*6, 7*). Thus, the transformation of benign prostate cells into malignant required a variety of metabolic alteration made the research is in the metabolism of prostate cancer is an active area for investigation (*8*).

Knowingly that one of the cancer hallmarks is the high glucose uptake and lactate release presented as what is known as the Warburg effect (*9*). The ability of cancer cells to metabolically adapt to different stress alterations and conditions helped cancer cells survive the common

hypoxic condition known to exist in most cancer cells and support their anabolic requirements (*10, 11*). Targeting the Warburg effect in prostate cancer is challenging due to the extensive network that regulates it.

One of the vital proteins controlling the Warburg effect is ENO1, which has a significant role in cell glycolysis, growth, migration, and invasion (*12, 13*). ENO1 is upstream of AKT and involved in its activation (*14*); ENO1 could also regulate the AMPK/mTOR signaling pathway and promote tumorigenesis and metastasis (*13*). ENO1 requires several activation strategies, one of which is through HIF-1 (*15*), also, SIX1, which is a major transcription regulator of ENO1 and a primary transcription regulator of the Warburg effect (*16*). Recent reports suggested that SIX1 overexpression is related to prostate cancer's progression and prognosis(*17*). Current reports also showed that SIX1 induce protein synthesis via the upregulation of mTOR (*18*).

Taken these findings together, we found investigating the possible linkage between SIX1/ ENO1 and AKT/ mTOR might propose a feasible strategy in the treatment of prostate cancer. We also investigated the SBF-1 possible effect on SIX1/ ENO1 and AKT/ mTOR signaling in the treatment of androgen-independent prostate cancer.

2. Materials and methods

2.1 Reagents

SBF-1 steroidal glycoside, provided by the co-authors Prof. Biao Yu and Dr. Lijun Sun, and its structure presented in Fig. 1A. Anti-AKT, anti-p-AKT$_{S473}$, anti-mTOR, anti-p-mTOR$_{S2481}$, anti-SIX1, anti-ENO1, and anti-Bcl-2 antibodies were purchased from Cell Signaling Technology (Beverly, MA). Anti-Lamin B1 and anti-GAPDH were purchased from Santa Cruz Biotechnology (Santa Cruz, CA). (3-(4,5-Dimethylthiazol-2-yl)-2,5-Diphenyltetrazolium

Bromide) (MTT) Moreover, dimethyl sulfoxide (DMSO) were obtained from Sunshine Biotechnology (Nanjing, China). All the plasmids, including pcDNA3.1 GFP-ENO1, GFP-mTOR, and mCherry-SIX1, were purchased from Gene-Script (Nanjing, China). All other chemicals obtained from Sigma-Aldrich (St. Louis, MO).

2.3 Cell culture

Human prostate cancer cell lines DU145 and PC3 cell lines obtained from Shanghai Institute of Cell Biology (Shanghai, China). All of the cells were maintained in DMEM medium (Life Technologies, Grand Island, NY) supplemented with 10% fetal bovine serum (FBS, Life Technologies), 100 U/mL penicillin, and 100 μg/mL streptomycin. All cell lines have been tested clear from mycoplasmas presence.

2.4 MTT assay

1×10^5 cells were seeded into 96-well plates and incubated with various concentrations of SBF-1 for indicated periods. The survival rate was detected, as described previously (*4*). MTT assay has been performed in triplicate.

2.5 Apoptosis, cell cycle, ROS, and cell adhesion assay

Cell apoptosis was determined by annexin V/PI staining. 1×10^6 of each cell line were measured by flow cytometry after the addition of FITC-conjugated annexin V and PI, as previously described (*19*). Annexin V^+ / PI^- and annexin V^+ / PI^+ considered as apoptotic cells in the early and late phases, respectively. Samples were analyzed by flow cytometry on a FACScan (Becton Dickinson).

For cell cycle analysis, cells were stained with propidium iodide (PI) as described in (*20*), and the cell cycle distribution was analyzed by flow cytometry on a FACScan (Becton Dickinson). The percentages of cells in G0/G1, S, and G2 phases were counted and compared. Cell adhesion and ROS assays were performed as reported in (*4*). All assays have been performed in triplicates.

For cell adhesion, 96-well flat-bottom plates were coated with 50 ml fibronectin (10 mg/ml) in PBS overnight at 4 8C and then blocked with 0.2% bovine serum albumin (BSA) for 2 h at room temperature followed by washing three times. Cells were added into each well in triplicate and incubated for 30 min at 37 8C. Plates were then washed three times with PBS to remove unbound cells. The numbers of cells that remained bound to the plates were analyzed by MTT assay. After subtraction of the background cell binding to BSA-coated wells, the percentage of adherent cells was calculated by dividing the optical density of the adherent cells by that of the initial input cells.

2.6 Western blot

Cells were lysed in lysis buffer, as described previously (*21*). The whole-cell lysates were collected and separated by 10% SDS-PAGE and subsequently electro-transferred onto a polyvinylidene difluoride membrane (Millipore Corp., Bedford, MA). The blocked membrane was incubated with the indicated antibodies, and final detection was performed using a chemiluminescent substrate system (Cell signaling, CA). All experiments have been performed in triplicates.

2.7 RNA extraction, reverse transcription PCR

Real-time PCR was performed as reported in (*22*). GAPDH used as a loading control. The primer sequences used in this study were as follows:

ENO1: forward, 5′- TGGTGTCTATCGAAGATCCCTT-3′;

reverse, 5′- CCTTGGCGATCCTCTTTGG-3′;

SIX1: forward, 5′- ACAAGAACGAGAGCGTACTCA-3′;

reverse, 5′- CTCCACGTAATGCGCCTTCA-3′;

β-actin: forward, 5′-CATGTACGTTGCTATCCAGGC-3′;

reverse, 5′-CTCCTTAATGTCACGCACGAT-3′.

All experiments have been performed in triplicates.

2.8 Gene silencing

PC3 or DU145 cells were seeded into six wells plate at a confluence of 1×10^6 and then transfected with the siRNA using Lipofectamine RNAi MAX (Thermo Scientific) according to the manufacturer protocol, the following sequences used for siRNA as follows:

mTOR sense: 5'- GCUCGUAAGUUGGGAUAACA-3',

SIX1sense: 5’- AGUUUGAGCUCCUGGCGUG-3’,

Control sequence sense: 5’-UGCCGUUCUUCAACGAGGA-3’.

The siRNA oligonucleotides, together with the corresponding antisense oligonucleotides, were synthesized by Gene Script (Nanjing, China). All experiments have been performed in triplicates.

2.9 Microscale thermophoresis (MST)

GFP-mTOR and mCherry-SIX1 constructs were purchased from Gene-Script (China). Each construct was transfected into 2×10^7 HEK293T cells, then cells were lysed in 1000 µl lysis buffer, including a protease inhibitor. The lysate was further centrifuged at 15,000 RPM to remove large aggregates. The concentration of GFP-mTOR was kept constant at 10 nM. mCherry-SIX1 has been titrated 1:1 dilutions, and its highest concentration was 880 nM. Monolith NT.115 was used to determine the binding affinity. All experiments have been performed in triplicates.

2.10 Confocal microscopy imaging

HEK293T cells were seeded in a 24-well plate (5×10^4 cells/well) and cultured for 24 h. After 24 h, the cells were transfected with either GFP-mTOR or mCherry-SIX1 for another 24 h. Then the cells are fixed using 4% paraformaldehyde. Next, 0.1% Triton X-100 is used for cell permeabilization, and 5% goat serum is used for blocking for 30 min. Cells were further incubated overnight with primary antibodies against mCherry (SIX1) (anti-mouse, 1:100, Santa Cruz, USA), GFP (mTOR) (anti-rabbit, 1:100, Proteintech, China). The next day, cells were incubated with either Alexa Fluor 594 or Alexa Fluor 488 for one h. Nuclei have been visualized with DAPI stain. The stained cells were examined with the FV10-ASW cell image system. All cell imaging and analysis have been done in triplicates.

2.11 Statistical analysis

Data were expressed as means ± SEM. The Student's *t*-test was used to evaluate the difference between groups. $P<0.05$ was considered significant. All in vitro data were generated from at least three independent experiments.

3. Results

3.1 SBF-1 exhibited potent cytotoxicity toward prostate cancer cell lines DU145 and PC3

DU145 and PC3 cells incubated with different concentrations of SBF-1 for 3 h. As a result, SBF-1 showed very strong cytotoxicity towards DU145 and PC3 cells Fig. 1B.

After incubating the cells with different doses of SBF1, cells were collected and subjected to analysis of the adhesive ability to fibronectin and laminin. SBF-1 showed significant inhibition on the adhesive ability of DU145 and PC3+ cells to fibronectin and laminin in a concentration-dependent manner Fig. 1C.

Next, we determined the percentage of apoptotic cells, as shown in Fig. 1D. Compared with the control, the percentage of apoptotic cells significantly increased in SBF-1-treated DU145 and PC3 cells. Besides, SBF-1 induced an increase in the ROS in both cell lines DU145 and PC3 Fig. 1E.

3.2 SBF-1 down-regulated ENO1 and its subsequent AKT/mTOR signaling

Considering the link between the SIX1/ENO1 and AKT/mTOR pathways, we further examined the effect of SBF-1 on those two pathways and possible outcomes under different stimulants. As shown in Fig. 2A. SBF-1 down-regulated AKT/mTOR and its downstream signaling as well as the SIX/ENO1. SBF-1 significantly reduced the protein levels of p-$AKT_{S473,}$ p-$mTOR_{S2481,}$ ENO1, and Bcl-2, while there was no effect on AKT, mTOR, and SIX1 protein levels.

From the above results, we hint that SBF-1 directly affects one of the major vital proteins in the metabolic pathway, ENO1/AKT/mTOR. Hence, we used glucose and Diphenyleniodonium

(DPI) independently to stimulate DU145 and PC3 cells metabolism, this is to achieve a change in the ENO1 levels as it is known to be a key regulator in the cellular metabolism. We compared the effect of SBF-1 on the SIX1/ENO1 axis and the AKT/mTOR pathway in the presence or absence of DPI. As shown in Fig. 2B. SBF-1 reduced the protein levels of p-$AKT_{S473,}$ p-$mTOR_{S2481,}$ ENO1, and Bcl-2, while there was no effect on the protein levels of AKT, mTOR, and SIX1 in the presence or absence of DPI. At the same time, DPI only affects the protein level of p-$AKT_{S473,}$ p-$mTOR_{S2481,}$ with no effect on ENO1. These results suggest that SBF-1 does target the upstream of the AKT/mTOR pathway and that ENO1 might be a consensus target of SBF-1.

ENO1 is an essential protein in cellular glycolysis. So, we stimulated PC3 and DU145 cells using glucose, which is known to be regulated through the glycolysis enzyme ENO1, and it is also a contributor to the regulation of the Warburg effect (*12*). As shown in Fig. 2C, SBF-1 reduced the protein levels of p-$AKT_{S473,}$ p-$mTOR_{S2481,}$ ENO1, and Bcl-2, while there was no effect on the protein levels of AKT, mTOR, and SIX1. From this result, we indicated that SBF-1 could directly target the cellular metabolism presented in its vital regulator, ENO1. We further focused the study on the SBF-1 effect on ENO1 regulation. Next, we checked the gene expression of ENO1 and its transcription regulator SIX1. As shown in Fig. 2D, SBF-1 significantly reduced the ENO1 gene expression with no effect on SIX1 gene expression. From the above results, we indicated that SBF-1 affect the prostate cancer cell metabolism through a key protein ENO1, the further analysis shall clarify the mode of how SBF-1 inhibits the growth of prostate cancer cell lines DU145 and PC3 through this major key protein ENO1.

3.3 SBF-1 down-regulated ENO1 through attenuation of SIX1/ENO1 axis

Next, we analyzed how SBF-1 inhibited ENO1. SIX1 known to regulate the gene expression of ENO1. Also, the overexpression of SIX1 is related to the ENO1 reporter activity (*16*). Previously, reports shown SIX1 to induce protein synthesis signaling mainly via the up-regulation of mTOR (*18*). Also, mTOR inhibition significantly impaired the mRNA expression of crucial glycolysis gene ENO1 (*23*). Together, these data suggest that SIX1 and mTOR may involve in the regulation of ENO1. SBF-1 reduced the protein levels of p-mTOR$_{S2481}$ and ENO1 in the presence or absence of SIX1 silencing while silencing SIX1 alone did not affect p-mTOR$_{S2481}$ or ENO1 protein levels. Also, there was no change in mTOR levels Fig. 3A. We determined ENO1 gene expression in the presence or absence of SBF-1 while silencing SIX1. SBF-1 significantly reduced the gene expression of the ENO1 gene in the case of silencing SIX1. Silencing SIX1 alone did not cause any change to the ENO1 gene expression Fig. 3B.

Next, we silenced mTOR in DU145 and PC3 cells, and the effect of SBF-1 was examined. With or without silencing mTOR, SBF-1 inhibited the ENO1 protein level. Also, silencing mTOR in the absence of SBF-1 inhibited the ENO1 protein level, while there was no change in the level of SIX1 Fig. 3C. Besides, silencing mTOR in the presence or absence of SBF-1 significantly reduced ENO1 gene expression Fig. 3D.

From the previous result, we concluded that mTOR might be a vital member in the regulation of ENO1, and we further analyzed the ENO1 expression level using mTOR inhibitor, Rapamycin. As shown in Fig. 3E, SBF-1 inhibited ENO1 and p-mTOR$_{S2481}$ protein levels without affecting mTOR or SIX1 protein levels, while Rapamycin inhibited p-mTOR$_{S2481}$ protein level without affecting ENO1, mTOR, and SIX1. We further analyzed the ENO1 gene expression in both cell lines. Compared with the effect of SBF-1 on ENO1 gene expression, Rapamycin significantly reduced ENO1 gene expression Fig. 3F.

From the above data, we can conclude that mTOR is a major partner protein with SIX1 involved in the ENO1 regulation. Also, ENO1 gene expression and protein synthesis seem to have different paths. SBF-1 successfully inhibited both ENO1 gene expression and protein synthesis, while Rapamycin only affects ENO1 gene expression.

3.4 Nuclear mTOR is essential for the regulation of ENO1

Previously, we demonstrated that mTOR is involved with SIX1 in the regulation of ENO1. As known, SIX1 localized mainly in the nucleus, which was considered a master transcriptional regulator in prostate cancer (*23*), we further investigated if nuclear mTOR is vital for the ENO1 regulation.

In both DU145 and PC3 cell lines, SBF-1 mildly translocates mTOR from the nucleus into the cytoplasm. In contrast, adding nuclear import inhibitor INI-43 with SBF-1, mTOR completely shuttled into the cytoplasm; on the other hand, Rapamycin did not seem to affect the balance of the cytoplasmic and nuclear mTOR. However, adding INI-43 with Rapamycin, mTOR completely translocated into the cytoplasm Fig. 4A.

Next, we checked the ENO1 gene expression level in the case of INI-43. As shown in Fig. 4B. SBF-1 and Rapamycin significantly deduced the gene expression of ENO1 in the presence of INI-43.

Furthermore, we checked the protein expression level of ENO1 while adding INI-43 with either SBF-1 or Rapamycin. SBF-1 successfully inhibited the protein level of ENO1in the presence of INI-43, while Rapamycin failed to cause any change in the ENO1 protein level Fig. 4C.

We further analyzed the effect of ENO1 overexpression in prostate cancer cell lines DU145 and PC3 and the emerging effect of SBF-1 and Rapamycin on this overexpression. As shown in Fig. 4D. We transfected ENO1 overexpressing plasmid into DU145 and PC3 cell lines for 36 h then the expression has been monitored using confocal microscopy imaging. After confirming the overexpression of ENO1 in both cell lines DU145 and PC3, DU145 and PC3 cells treated with either SBF-1 100 nM or Rapamycin 50 nM for six h. SBF-1 successfully inhibited p-AKT_{S473}, p-$mTOR_{S2481}$, and Bcl-2 protein expressions. At the same time, there was no effect on the protein levels of AKT and mTOR. Meanwhile, overexpressing ENO1 reversed Rapamycin's inhibitory effect, and the protein levels of p-AKT_{S473}, p-$mTOR_{S2481}$, and Bcl-2 remained unchanged compared to the control group Fig. 4E.

From the above result, we hint that nuclear mTOR has a major significant role in the regulation of the ENO1 gene. Also, SBF-1 might have a better mode of action than Rapamycin in the inhibition of ENO1 protein level and gene expression, and it might include affecting the nuclear importing system of mTOR along with other mechanisms.

3.5 SBF-1 interrupted the interaction between mTOR and SIX

As shown in Fig. 5A. In silico analysis of the interaction between mTOR and SIX1 showed a significant binding affinity between mTOR and SIX1 (data not shown). The binding affinity for the interaction between GFP-mTOR and mCherry-SIX1 determined using Monolith NT.115, as mentioned in the methods. The fitting curve indicated a strong bind affinity between GFP-mTOR and mCherry-SIX1 at 7.8 nM. Next, we tested the effect of SBF-1 compared to Rapamycin on this interaction using confocal microscopy analysis. HEK293T transfected with GFP-mTOR and mCherry-SIX1 were incubated with SBF-1 100 nM and Rapamycin 50 nM for

six h. As shown in Fig. 5B, SBF-1 blocked the interaction between mTOR and SIX, while Rapamycin did not affect this interaction.

Immunoprecipitation further confirmed that SBF-1 blocked the interaction between mTOR and SIX1. At the same time, SBF-1 mildly shuttle mTOR from the nucleus to the cytoplasm Fig. 5C.

We further confirmed the interaction between mTOR and SIX1 through the construction of the ENO1 biotinylated promoter (1-350 bp). We performed DNA pull-down assay, as shown in Fig. 5D. After transfecting HEK293T cells with ENO1 construct, cells were treated with either SBF-1 100 nM or Rapamycin 50 nM for six h in the presence or absence of INI-43. The results showed that SIX1 conjugated with ENO1 promoter in all cases of treatment. At the same time, mTOR does not appear in the pulled down promoter while treated with SBF-1 or SBF-1 combined with Rapamycin in the presence of INI-43, indicating that SBF-1 did block the interaction between mTOR and SIX1 and that nuclear mTOR is a vital binding partner with SIX1 in the transcription of ENO1 Fig. 5E. Also, cells' nuclear extract has been taken and immunoprecipitated against SIX1, checking mTOR, and SIX1 interaction in the presence of SBF-1 or Rapamycin. SBF-1 entirely blocked the interaction between SIX1 and mTOR, while Rapamycin failed to do so Fig. 5F.

Taken together these data, we can conclude that blocking the interaction between mTOR and SIX1 could be a better strategy for the inhibition of ENO1 protein levels and gene expression.

4. Discussion

In our study, we found a novel treatment strategy for androgen-independent prostate cancer. As we know, prostate cancers in the early stage rely on androgens for growth and survival, and

androgen withdrawal therapy causes them to recede. Failed surgeries in the treatment of prostate cancer develop an anti-androgen resistance as the cancer cells become androgen-independent as a sort of acquired resistance mechanism—also, scientists identified AR-negative cell populations presented in Castration-Resistant Prostate Cancer (CRPC). Thereby, the need for Identification of new therapeutic strategies to target both AR-positive and AR-negative prostate cancer cells could enhance the survival mechanisms and would provide an approach to eliminate CRPC cells with the potential for synthetic lethality (*24, 25*).

Tumor cells known to uptake high glucose levels for energy consumption and proliferation compared to healthy cells (*26*). Interestingly, cancer cells could favor glycolysis over the more energetically efficient, oxidative phosphorylation. Even in aerobic conditions, cancer cells prefer glycolysis because it is beneficial for proliferating by generating other metabolites (*27*). This phenomenon is known as the "Warburg effect," currently it is widely established a promising strategy for specific tumor targeting through attenuating the Warburg effect. We tested SBF-1, which showed a robust anti-tumor effect on Androgen independent DU145 and PC3 prostate cancer cell lines and checked its mode of action toward the inhibition of those cells' growth.

Knowingly that SIX1 is usually a developmental restricted transcriptional regulator and frequently dysregulated in multiple cancers. Increasing evidence shows that overexpression of SIX1 plays a crucial role in tumorigenesis. Also, the Increased expression of SIX1 correlates with the progression and prognosis of prostate cancer (*17*). While the role of SIX1 in prostate cancer is still relatively new, scientists identified SIX1 as a major transcription regulator of the Warburg effect and other cellular functions in prostate cancer (*16*). As far, linking the SIX1/ENO1 axis and AKT/mTOR pathway comes from a critical protein in the cellular functions, ENO1, it has a significant role in the cell glycolysis, growth, migration, and invasion

(*12, 14, 28, 29*). It is also known to promote tumorigenesis and metastasis via regulating the AMPK/mTOR pathway (*13*).

PI3K-AKT-mTOR signaling axis plays a critical role in the development and maintenance of CRPC. This pathway deregulated in most of the advanced prostate cancer. Also, its signaling axis serves as a critical connection for the integration of growth signals. This pathway with downstream cellular processes such as protein synthesis, proliferation, survival, metabolism, and differentiation allows cancer cells to adapt to the stress resulting from androgen withdrawal and develop mechanisms to overcome it (*30*). Targeting the linkage between those two critical pathways theorizes a feasible strategy for prostate cancer treatment. Reports have shown that nuclear mTOR act as a transcriptional integrator of the androgen signaling pathways in prostate cancer (*23*). We know that mTOR inhibition using Rapamycin did not affect the expression of SIX1, but the upregulation of mTOR induces protein synthesis signaling (*18*). Those findings aided by our previous results found that mTOR has direct interaction with SIX1 protein for the first time.

SBF-1 downregulated AKT/mTOR pathway and inhibited the protein levels of p-AKT_{S473}, p-$mTOR_{S2481,}$ and Bcl-2, a major pathway in the Androgen independent resistance mechanisms (*30*). Also, SBF-1 decreased the protein level of ENO1, a major essential protein in the Warburg effect (*12*). Taken together with those finding, we assumed that ENO1 might be a significant target of SBF-1, especially we know that the negative regulator of the Warburg effect.

Warburg effect aid cancer cells with proper metabolic function due to the massive energy consumption of cancer cells. Thus, stimulating the cells with glucose will interfere with the Warburg effect, especially the glycolysis enzyme ENO1. The result of treating the cells with SBF-1 after being stimulated with glucose has shown inhibition of p-AKT_{S473}, p-$mTOR_{S2481}$,

ENO1, and Bcl-2. From these results, we indicated that SBF-1 might affect cell metabolism. Furthermore, SBF-1 shown to induce an increase in the ROS levels Fig. 1E. ROS levels linked to the Warburg effect (*31*). Thus, we stimulated DU145 and PC3 cell lines with DPI to increase ROS levels (*32*). Interestingly, stimulating the cells with DPI reduced the protein levels of p-AKT_{S473}, p.$mTOR_{S2481.}$ In contrast, with no effect on ENO1 protein, while SBF-1, along with DPI, caused the inhibition of ENO1 protein, taken this result, we assumed that ENO1 might be the target of which SBF-1 caused the inhibition of the cell growth.

Following ENO1 role in prostate cancer and its vital role in the Warburg effect, we found that nuclear mTOR is essential for the transcription of ENO1 but not its translation, furthermore for the first time to identify that mTOR bind to SIX1 and act as a coregulator for gene transcription, i.e., ENO1.

At last, SBF-1 blocked the interaction between mTOR and SIX1, resulting in better inhibition of ENO1 protein and gene expression levels. We hypothesize that nuclear mTOR is critical for the transcription of ENO1. Also, the cytoplasmic mTOR and SIX1 may have a role in the ENO1 translation. Blocking the interaction between mTOR and SIX1 in the nucleus and the cytoplasm by SBF-1 gave a better inhibition of ENO1 protein and gene expression. SBF-1, in this case, shown better outcomes than novel mTOR inhibitor Rapamycin, it appeared as the overexpression of ENO1 reversed the effect of Rapamycin but not SBF-1. Our results showed that targeting ENO1 in androgen-independent prostate cancer cells is smart in treating prostate cancer and its form of resistance. Also, the blockade of the interaction between mTOR and SIX1 will altogether signify the inhibition of ENO1, resulting in a better outcome of the inhibition of prostate cancer cells.

Here we present a novel small molecule SBF-1 that showed a remarkable and novel strategy for prostate cancer treatment, which promises to overcome prostate cancer resistance.

Conclusion

Our study has revealed that SBF-1 is a potent anti-tumor agent in prostate cancer treatment. Furthermore, nuclear mTOR is a critical key partner of SIX1 in regulating ENO1 protein and gene expressions. Also, attenuation of the interaction between mTOR and SIX1 is a better path for the down-regulation of ENO1 and better outcomes in the treatment of AR-independent prostate cancer. Our study provided an insight into a new mechanism that controls the Warburg effect and its critical regulatory protein, ENO1. Future investigations shall reveal the potential of this new interaction between mTOR and SIX1 and its feasibility in treating prostate cancer.

Acknowledgments

This study was supported by the National Natural Science Foundation of China (No. 81730100, 21937005), Six Talents Peaks in Jiangsu Province (YY-004), Fundamental Research Funds for the Central Universities and Technological innovation funding of Nanjing University.

Conflict of interest statement

The authors have declared no conflict of interest.

References

1. Litwin MS, Tan HJ. The Diagnosis and Treatment of Prostate Cancer: A Review. JAMA. 2017; 317:2532-2542.

2. Litvinov IV, Antony L, Dalrymple SL, Becker R, Cheng L, Isaacs JT. PC3, but not DU145, human prostate cancer cells retain the coregulators required for tumor suppressor ability of androgen receptor. Prostate. 2006; 66:1329-1338.

3. Li W, Ouyang Z, Zhang Q, Wang L, Shen Y, Wu X, Gu Y, Shu Y, Yu B, Wu X, Sun Y, Xu Q. SBF-1 exerts strong anticervical cancer effect through inducing endoplasmic reticulum stress-associated cell death via targeting sarco/endoplasmic reticulum Ca(2+)-ATPase 2. Cell Death Dis. 2014; 5:e1581.

4. Li W, Song R, Fang X, Wang L, Chen W, Tang P, Yu B, Sun Y, Xu Q. SBF-1, a synthetic steroidal glycoside, inhibits melanoma growth and metastasis through blocking interaction between PDK1 and AKT3. Biochem Pharmacol. 2012; 84:172-181.

5. Elgehama A, Chen W, Pang J, Mi S, Li J, Guo W, Wang X, Gao J, Yu B, Shen Y, Xu Q. Blockade of the interaction between Bcr-Abl and PTB1B by small molecule SBF-1 to overcome imatinib-resistance of chronic myeloid leukemia cells. Cancer Lett. 2016; 372:82-88.

6. Twum-Ampofo J, Fu DX, Passaniti A, Hussain A, Siddiqui MM. Metabolic targets for potential prostate cancer therapeutics. Curr Opin Oncol. 2016; 28:241-247.

7. Sadeghi RN, Karami-Tehrani F, Salami S. Targeting prostate cancer cell metabolism: impact of hexokinase and CPT-1 enzymes. Tumour Biol. 2015; 36:2893-2905.

8. Eidelman E, Twum-Ampofo J, Ansari J, Siddiqui MM. The Metabolic Phenotype of Prostate Cancer. Front Oncol. 2017; 7:131.

9. Hanahan D, Weinberg RA. Hallmarks of cancer: the next generation. Cell. 2011; 144:646-674.

10. Iqbal MA, Gupta V, Gopinath P, Mazurek S, Bamezai RN. Pyruvate kinase M2 and cancer: an updated assessment. FEBS Lett. 2014; 588:2685-2692.

11. Gatenby RA, Gillies RJ. Why do cancers have high aerobic glycolysis? Nat Rev Cancer. 2004; 4:891-899.

12. Capello M, Ferri-Borgogno S, Riganti C, Chattaragada MS, Principe M, Roux C, Zhou W, Petricoin EF, Cappello P, Novelli F. Targeting the Warburg effect in cancer cells through ENO1 knockdown rescues oxidative phosphorylation and induces growth arrest. Oncotarget. 2016; 7:5598-5612.

13. Zhan P, Zhao S, Yan H, Yin C, Xiao Y, Wang Y, Ni R, Chen W, Wei G, Zhang P. alpha-enolase promotes tumorigenesis and metastasis via regulating AMPK/mTOR pathway in colorectal cancer. Mol Carcinog. 2017; 56:1427-1437.

14. Fu QF, Liu Y, Fan Y, et al. Alpha-enolase promotes cell glycolysis, growth, migration, and invasion in non-small cell lung cancer through FAK-mediated PI3K/AKT pathway. J Hematol Oncol. 2015; 8:22.

15. Zheng F, Jang WC, Fung FK, Lo AC, Wong IY. Up-Regulation of ENO1 by HIF-1alpha in Retinal Pigment Epithelial Cells after Hypoxic Challenge Is Not Involved in the Regulation of VEGF Secretion. PLoS One. 2016; 11:e0147961.

16. Li L, Liang Y, Kang L, et al. Transcriptional Regulation of the Warburg Effect in Cancer by SIX1. Cancer Cell. 2018; 33:368-385 e367.

17. Zeng J, Shi R, Cai CX, Liu XR, Song YB, Wei M, Ma WL. Increased expression of Six1 correlates with progression and prognosis of prostate cancer. Cancer Cell Int. 2015; 15:63.

18. Wang H, Li X, Liu H, Sun L, Zhang R, Li L, Wangding M, Wang J. Six1 induces protein synthesis signaling expression in duck myoblasts mainly via up-regulation of mTOR. Genet Mol Biol. 2016; 39:151-161.

19. Azeem W, Hellem MR, Olsen JR, Hua Y, Marvyin K, Qu Y, Lin B, Ke X, Oyan AM, Kalland KH. An androgen response element driven reporter assay for the detection of androgen receptor activity in prostate cells. PLoS One. 2017; 12:e0177861.

20. Sun Y, Wu XX, Yin Y, Gong FY, Shen Y, Cai TT, Zhou XB, Wu XF, Xu Q. Novel immunomodulatory properties of cirsilineol through selective inhibition of IFN-gamma signaling in a murine model of inflammatory bowel disease. Biochem Pharmacol. 2010; 79:229-238.

21. Guo W, Liu W, Chen Z, Gu Y, Peng S, Shen L, Shen Y, Wang X, Feng GS, Sun Y, Xu Q. Tyrosine phosphatase SHP2 negatively regulates NLRP3 inflammasome activation via ANT1-dependent mitochondrial homeostasis. Nat Commun. 2017; 8:2168.

22. Liu W, Wu TC, Hong DM, Hu Y, Fan T, Guo WJ, Xu Q. Carnosic acid enhances the anti-lung cancer effect of cisplatin by inhibiting myeloid-derived suppressor cells. Chin J Nat Med. 2018; 16:907-915.

23. Audet-Walsh E, Dufour CR, Yee T, et al. Nuclear mTOR acts as a transcriptional integrator of the androgen signaling pathway in prostate cancer. Genes Dev. 2017; 31:1228-1242.

24. Hoang DT, Iczkowski KA, Kilari D, See W, Nevalainen MT. Androgen receptor-dependent and -independent mechanisms driving prostate cancer progression: Opportunities for therapeutic targeting from multiple angles. Oncotarget. 2017; 8:3724-3745.

25. Feldman BJ, Feldman D. The development of androgen-independent prostate cancer. Nat Rev Cancer. 2001; 1:34-45.

26. Hossain F, Andreana PR. Developments in Carbohydrate-Based Cancer Therapeutics. Pharmaceuticals (Basel). 2019; 12.

27. Vander Heiden MG, Cantley LC, Thompson CB. Understanding the Warburg effect: the metabolic requirements of cell proliferation. Science. 2009; 324:1029-1033.

28. Wang L, Bi R, Yin H, Liu H, Li L. ENO1 silencing impaires hypoxia-induced gemcitabine chemoresistance associated with redox modulation in pancreatic cancer cells. Am J Transl Res. 2019; 11:4470-4480.

29. Qian X, Xu W, Xu J, Shi Q, Li J, Weng Y, Jiang Z, Feng L, Wang X, Zhou J, Jin H. Enolase 1 stimulates glycolysis to promote chemoresistance in gastric cancer. Oncotarget. 2017; 8:47691-47708.

30. Edlind MP, Hsieh AC. PI3K-AKT-mTOR signaling in prostate cancer progression and androgen deprivation therapy resistance. Asian J Androl. 2014; 16:378-386.

31. El Sayed SM, Mahmoud AA, El Sawy SA, Abdelaal EA, Fouad AM, Yousif RS, Hashim MS, Hemdan SB, Kadry ZM, Abdelmoaty MA, Gabr AG, Omran FM, Nabo MM, Ahmed NS. Warburg effect increases steady-state ROS condition in cancer cells through decreasing their antioxidant capacities (anticancer effects of 3-bromopyruvate through antagonizing Warburg effect). Med Hypotheses. 2013; 81:866-870.

32. Cross AR, Jones OT. The effect of the inhibitor diphenylene iodonium on the superoxide-generating system of neutrophils. Specific labelling of a component polypeptide of the oxidase. Biochem J. 1986; 237:111-116.

Figures

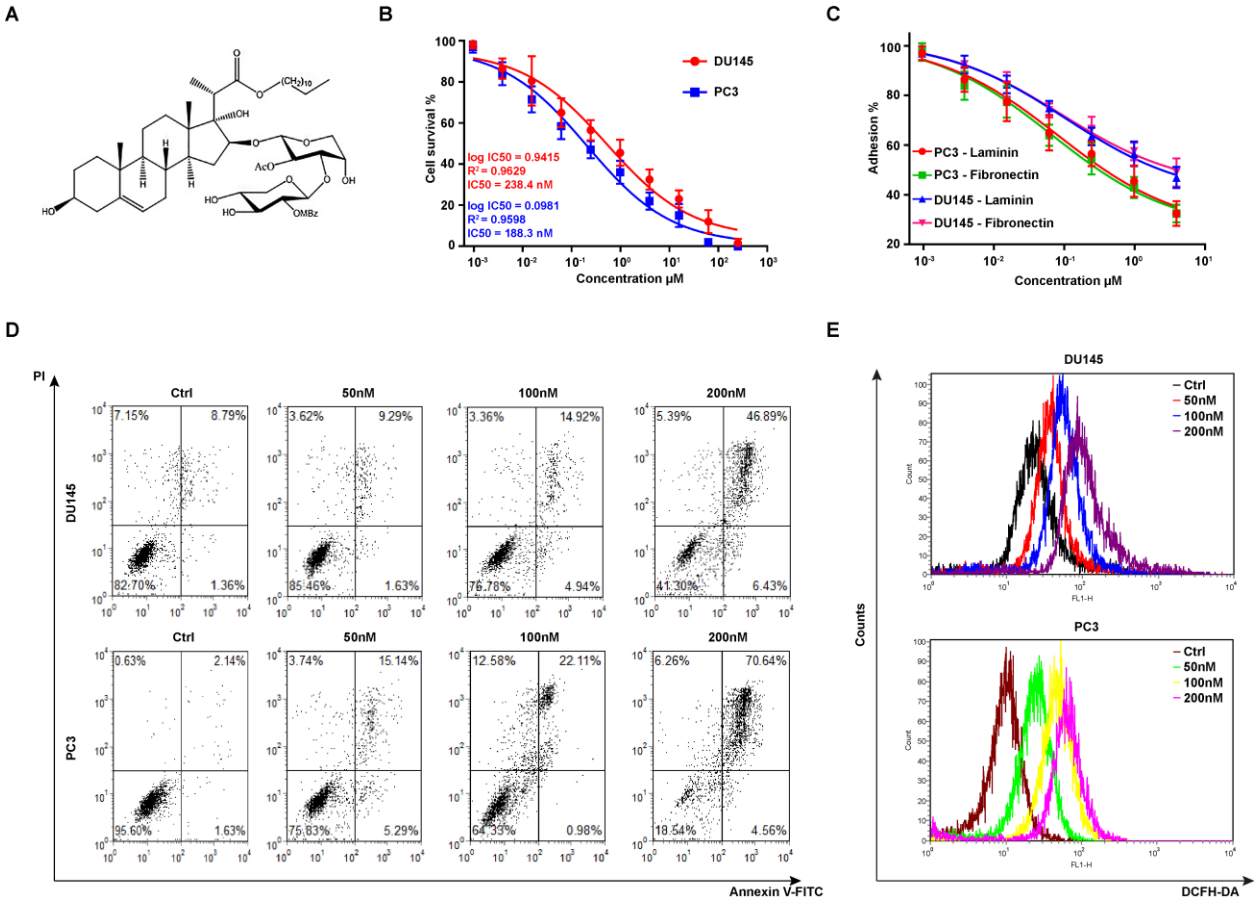

Fig. 1 SBF-1 inhibited proliferation, adhesion, and induced apoptosis and ROS levels elevation in DU145 and PC3 cells. (A) Structure of SNF-1 (B) 1 × 10^5 DU145 or PC3 cells were seeded into 96-well microplates; afterward, cells were incubated with various concentrations of SBF-1 for 24 h. Cell viability was determined by MTT assay. (C) Cell adhesive ability was tested toward fibronectin and laminin. (D) The percentages of apoptotic cells were determined by Annexin V/PI staining. (E) DU145 and PC3 cells have been treated with different doses of SBF-1; the ROS level has been determined using DCFH-DA staining. Values in A and B were shown as the mean ± SEM. Data in D-G were representative of three independent experiments.

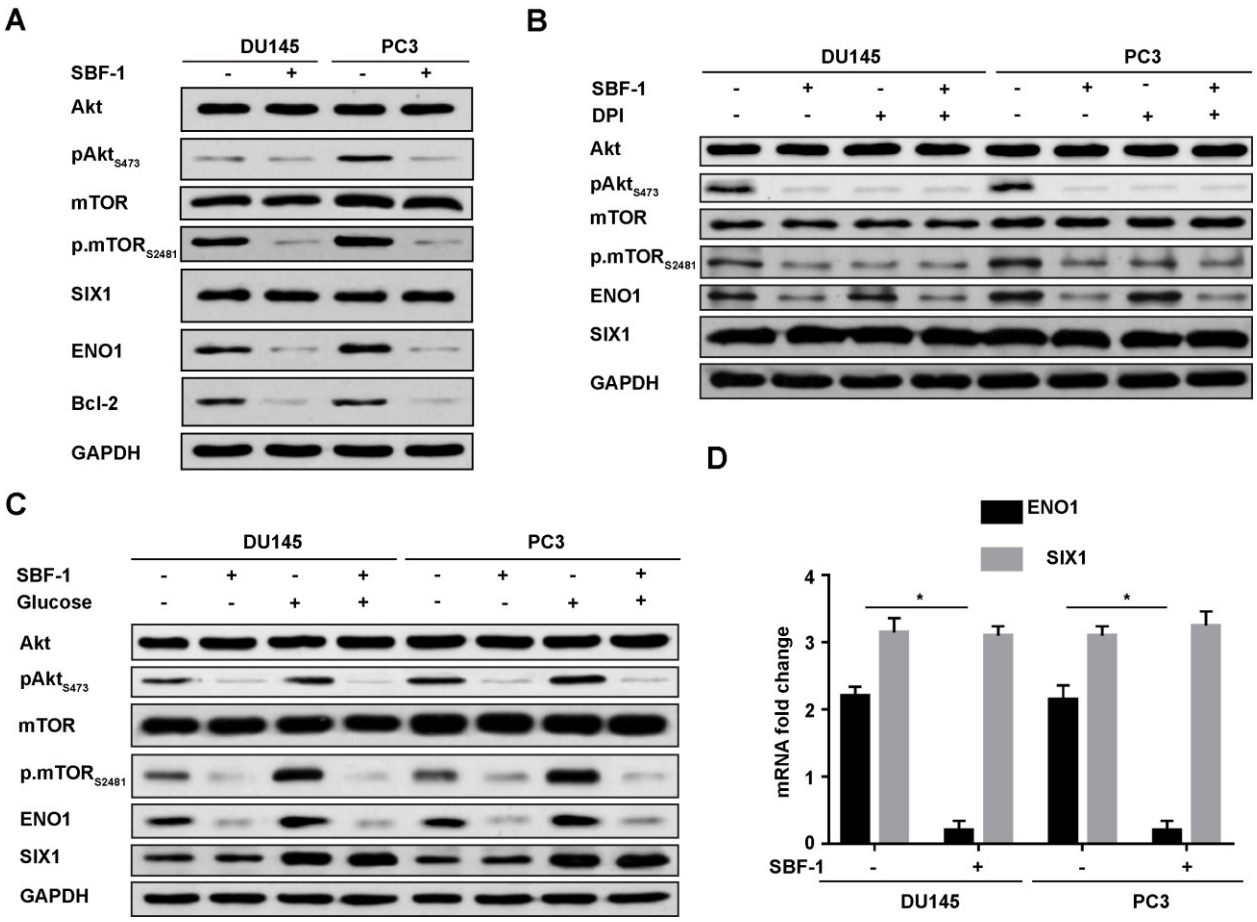

Fig. 2 SBF-1 inhibited AKT/mTOR pathway and decreased ENO1 expression. (A, B, and C) DU145 and PC3 cells were treated with SBF-1 for 6 h at 100 nM of final concentration in the presence or absence of glucose 5 nM or DPI 1 μM. The protein levels of AKT, p-AKT$_{S473}$, mTOR, p-mTOR$_{S2481}$, SIX1, ENO1, and Bcl-2 were determined in the whole lysate by western blot. GAPDH was used as a loading control. (D) DU145 and PC3 cells were treated with 100 nM SBF-1 for 6 h, and the mRNA levels of ENO1 and SIX1 were determined. Values in D were shown as the mean ± SEM of three experiments. *$P < 0.05$, **$P < 0.01$ vs as indicated. Data in A, B, and C were representative of three independent experiments.

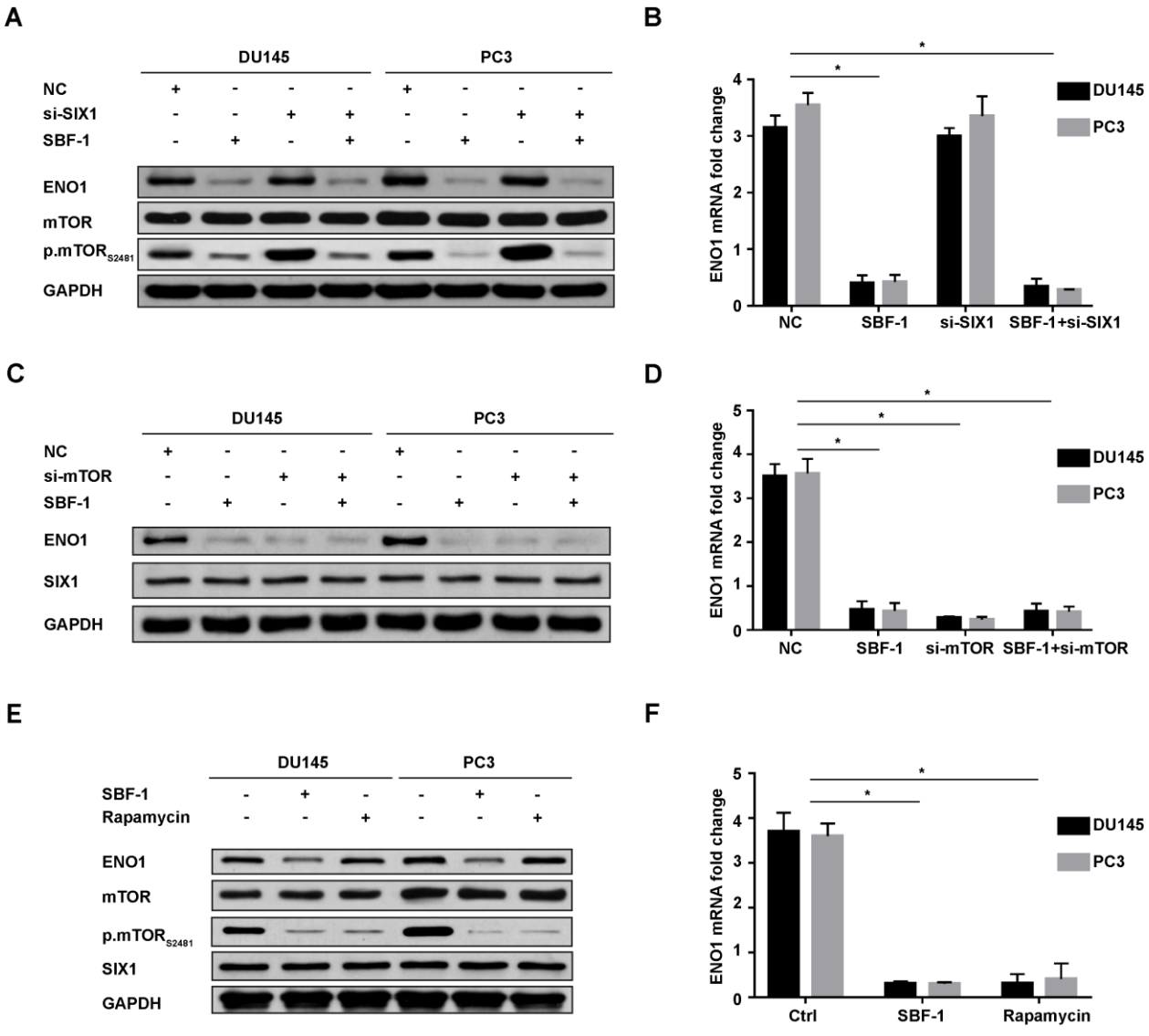

Fig. 3 mTOR was essential for ENO1 protein and gene expression. (A, C) SIX1 or mTOR was silenced independently in DU145 or PC3 cells. The effect of SBF-1 on ENO1, mTOR, and p.mTOR^{S2481} expressions was determined by western blot. (E) DU145 and PC3 cells were treated with SBF-1 for 6 h at 100 nM or Rapamycin 50 nM for 6 h. The protein levels of mTOR, p-mTOR$_{S2481}$, SIX1, and ENO1 were determined in the whole lysate by western blot, GAPDH has been used as a control. (B, D, F) The mRNA expression of ENO1 was determined by Q-PCR. Values in B, D, and F were shown as the mean ± SEM of three experiments. *$P < 0.05$, **$P < 0.01$ vs as indicated. Data in A, C, and E were representative of three independent experiments.

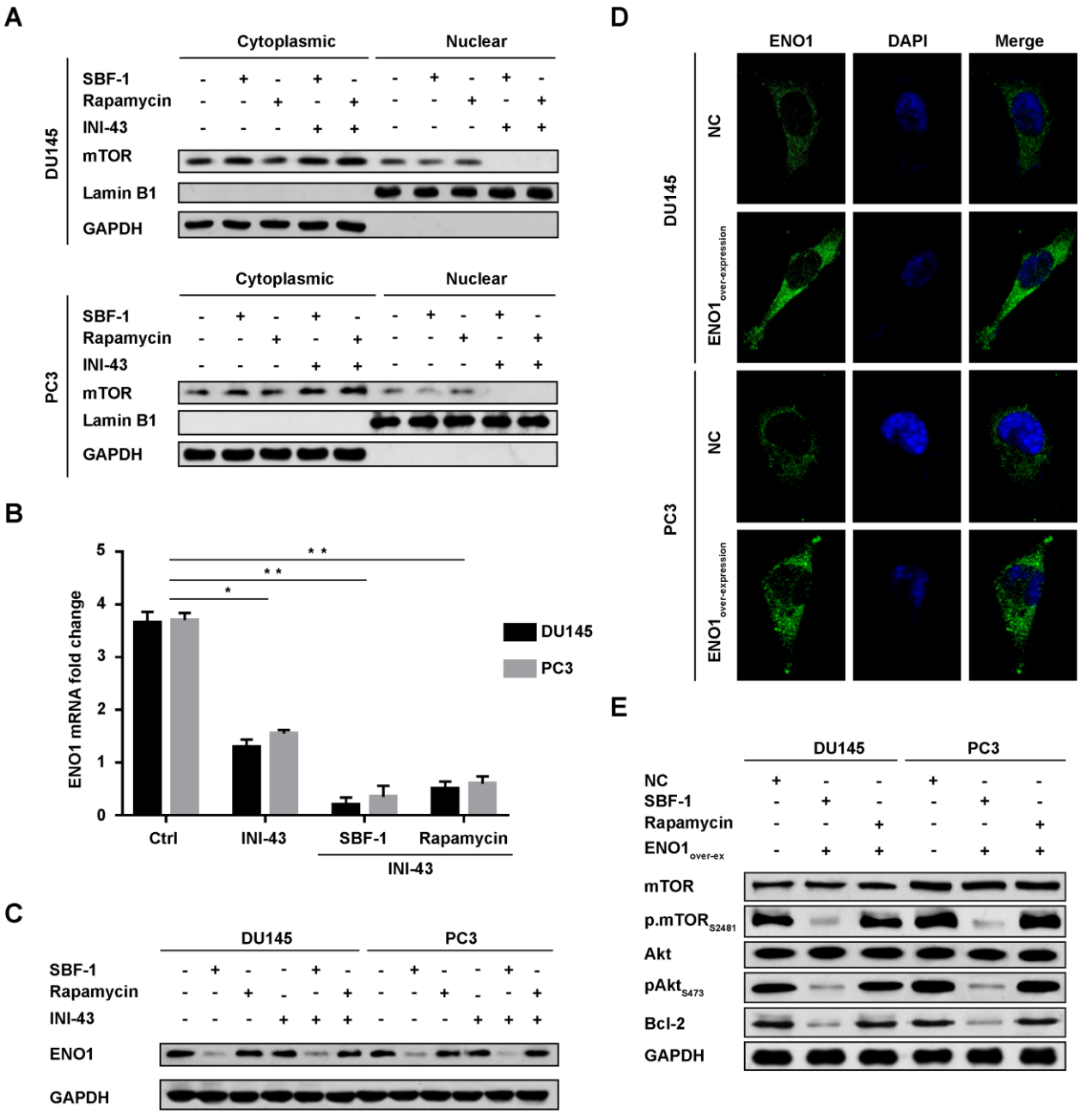

Fig. 4 Nuclear mTOR is required for ENO1 regulation. (A) DU145 and PC3 cells were treated with SBF-1 for 6 h at 100 nM or Rapamycin 50 nM for 6 h of final concentration in the presence or absence of INI-43 1 μM. the status of mTOR has been determined by western blotting after cell lysate being fractionated, Lamin B1, and GAPDH used as a loading control. (B)

Gene expression of ENO1 has been determined using Q-PCR. (C) DU145 and PC3 cells were treated with SBF-1 for 6 h at 100 nM or Rapamycin 50 nM for 6 h of final concentration in the presence or absence of INI-43 1 μM. the protein expression of ENO1 has been determined by western blotting, GAPDH used as a loading control. (D) pcDNA3.1 plasmid overexpressing ENO1 transfected into DU145, and PC3 cells, the expression of ENO1 has been determined using an FV10-ASW imaging system. (E) DU145 and PC3 cells were treated with SBF-1 for 6 h at 100 nM or Rapamycin 50 nM for 6 h of final concentration in the presence of ENO1 overexpressing cells. The protein levels of AKT, p-AKT_{S473}, mTOR, p-$mTOR_{S2481}$, and Bcl-2 were determined in the whole lysate by western blot. GAPDH was used as a loading control. Values in B were shown as the mean ± SEM of three experiments. *$P < 0.05$, **$P < 0.01$ vs as indicated. Data in A, C, and E were representative of three independent experiments.

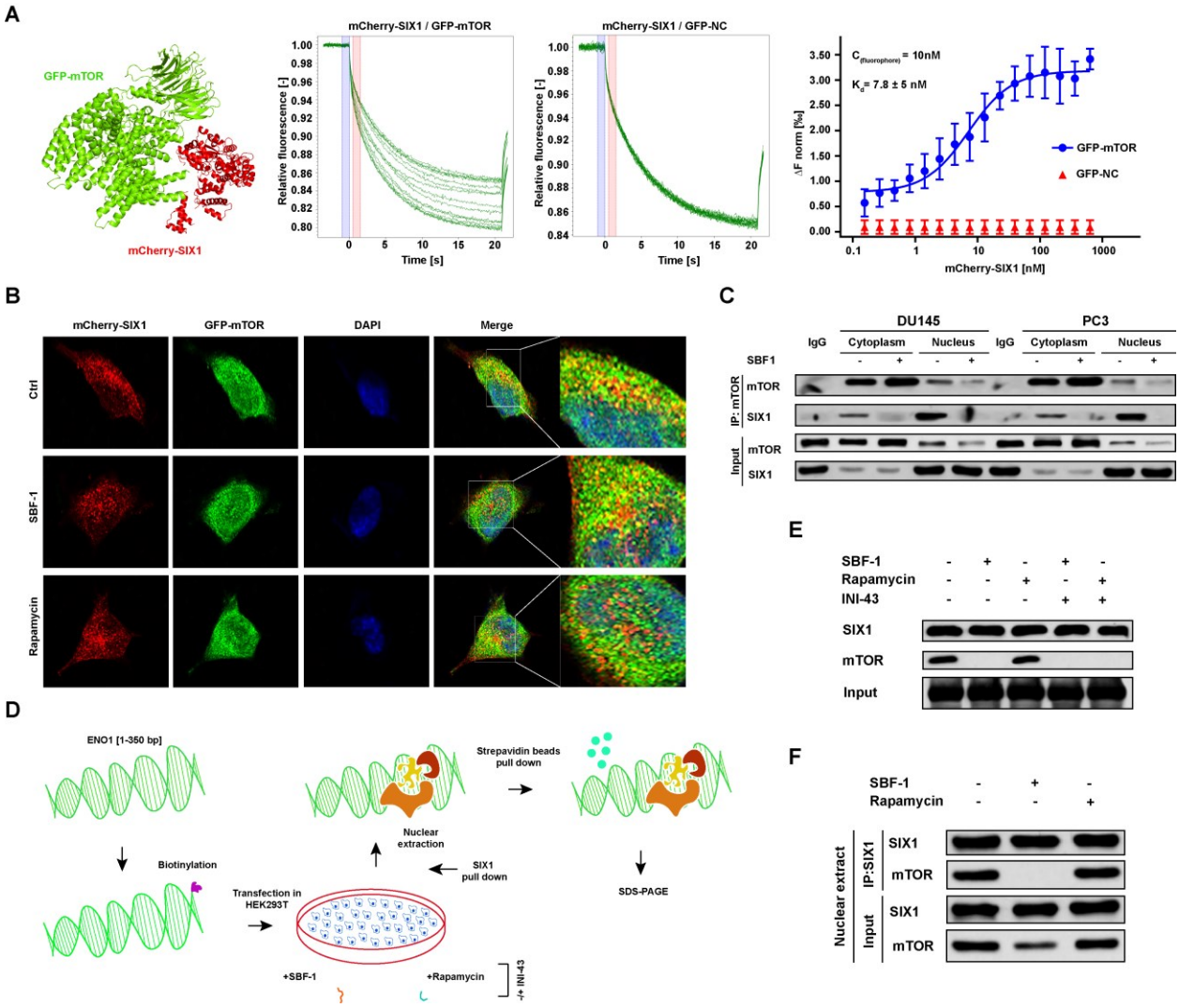

Fig. 5 mTOR bind to SIX1, SBF-1 block the interaction between mTOR and SIX1. (A) Purified GFP-mTOR at a final concentration of 10 nM has been incubated with different concentrations of purified mCherry-SIX1, and the binding affinity was determined as the change in the GFP fluorescence using MST assay. (B) GFP-mTOR and mCherry-SIX1 have been transfected into HEK293T, then the cells have been treated with 100 nM of SBF-1 for 6 h, or Rapamycin 50 nM for 6 h, then the interaction between mTOR and SIX1 has been determined using an FV10-ASW imaging system. (C) DU145 and PC3 cells were treated with SBF-1 for 6 h

at 100 nM. the interaction between mTOR and SIX1 has been determined by western blotting after cell lysate being fractionated. (D) Schematic diagram of DNA pulldown experiment design for ENO1 promoter. (E) ENO1 biotinylated construct has been transfected into HEK293T then the cells were treated with SBF-1 for 6 h at 100 nM or Rapamycin 50 nM for 6 h of final concentration in the presence or absence of INI-43 1 μM, the presence or mTOR and SIX1 has been determined using western blotting after ENO1 construct been precipitated. Biotin has been used as a control. (F) ENO1 biotinylated construct has been transfected into HEK293T then the cells were treated with SBF-1 for 6 h at 100 nM or Rapamycin 50 nM for 6 h of final concentration then interaction between mTOR and SIX1 has been determined using IP assay toward SIX1 in the nuclear extract. Data in A, B, C, and F were representative of three independent experiments.